Environmental Science and Pollution Research (2019) 26:672–683
https://doi.org/10.1007/s11356-018-3590-x

RESEARCH ARTICLE

Distilled pyroligneous liquor obtained from *Eucalyptus grandis* and chitosan: physicochemical properties of the solution and films

Fabiane Grecco da Silva Porto[1] · Ângela Diniz Campos[1] · Irene Teresinha Santos Garcia[2]

Received: 30 July 2018 / Accepted: 23 October 2018 / Published online: 9 November 2018

Abstract

The pyroligneous liquor is a product obtained during the production of charcoal, with well-known antimicrobial activity. In this work, we characterized the physical chemistry properties of a formulation composed of distilled pyroligneous liquor (DPL), obtained from *Eucalyptus grandis*, and chitosan. A good interaction between the polymer and the solvent was observed. Auto-supported films were prepared with these systems and characterized with respect to their structure and photo-protection properties, water vapor permeability, and resistance to water and to thermal degradation. They present a semi-crystalline structure and are hygroscopic, but are stable under immersion for up to 7 days. The swelling degree in water is 300% in weight and the permeability to water vapor was between 30 and 45 g m^{-1} h^{-1} (for films with 80 to 10 μm, respectively). The obtained films are able to efficiently block the incident UVB and UVC radiation; the molar absorptivity decreases exponentially with increasing wavelength and is stable up to 300 °C. These properties confer desirable properties to the films, obtained from these precursors of a renewable source, to be used as coatings.

Keywords Distilled pyroligneous liquor · *Eucalyptus grandis* · Chitosan · Colloidal systems · Films · Ultraviolet radiation · Protective coating

Introduction

The Brazilian agribusiness has an important source of renewable energy in the forestry sector. Currently, Brazil has 7.8 million hectares of forest plantation, approximately 72% of which is eucalyptus trees, of which 1.1 million hectares are exclusively destined for coal production. This charcoal is obtained by the partial burning of the wood in rudimentary furnaces and Brazil is one of the most important Mondial producers (Daroit et al. 2013; Pimenta et al. 2018). An important environmental problem occurs during the transformation of wood into coal, where greenhouse gases are generated, causing a negative social and environmental impact (Pereira et al. 2017). In the southern part of Brazil, the production of charcoal is an important activity for families of small farmers and thousands of charcoal kilns are spread over more than 10,000 small properties (Daroit et al. 2013; Furtado et al. 2015).

The environmental impact of greenhouse gas emissions can be reduced if these furnaces are adapted to collect a condensable fraction. This product is known as pyroligneous liquor, pyroligneous acid, wood vinegar, liquid smoke or bioleum, pyroligneous tar, pyrolysis oil, bio-crude oil, biofuel oil, liquid wood, wood oil, and wood distillates (Campos 2018; Pimenta et al. 2018).

Campos (2018) published technical recommendations for the construction of coal-fired furnaces adapted for the collection of pyroligneous acid for agricultural use. The pyroligneous acid obtained by this process has good quality and low tar content. Besides emission reductions, the increase in the application of this product can make it a source of alternative income (Almeida et al. 2017a, b).

The term pyroligneous originates from the words *pyrolysis*, the process involved, and *lignin*, one of the components of the plant biomass from which it is derived. We use the pyroligneous liquor (PL) as the general name to designate this product (Mathew and Zakaria 2015).

Responsible editor: Giovanni Benelli

Electronic supplementary material The online version of this article (https://doi.org/10.1007/s11356-018-3590-x) contains supplementary material, which is available to authorized users.

✉ Irene Teresinha Santos Garcia
Irene.garcia@ufrgs.br

[1] Laboratório de Fisiologia Vegetal, Embrapa Clima Temperado, Br 392, Km 78, caixa postal 403, Pelotas 96010-971, Brazil

[2] Departamento de Físico-Química, Instituto de Química, Universidade Federal do Rio Grande do Sul, Avenida Bento Gonçalves 9500, Porto Alegre, RS 91501-970, Brazil

The composition of PL mainly depends on the extraction temperature and also on the origin of the raw material. PL has a typical smell of smoke and a reddish-brown coloration (Lohri et al. 2017). A period of 4 to 6 months storage is necessary to stabilize this product, which is a complex, polar mixture composed of water, carboxylic acids, hydroxyaldehydes, hydroxyketones, alcohols, derivatives of furan and pyran, esters, phenolic compounds, carbohydrate derivatives, and nitrogen compounds, among others (Campos 2018; Lohri et al. 2017; Mathew and Zakaria 2015; Pimenta et al. 2018).

The antioxidant and antimicrobial characteristics of PL have been attributed to the organic acids and phenols present in its composition, so it is used as a preservative in cosmetic products and sterilizing agents (Almeida et al. 2017a; Souza et al. 2012). Due to its antimicrobial activity, PL also has been used for veterinary and agricultural purposes. It has a fertilizing effect on some plants and presents nematocidal, fungicidal, and insecticidal action in the control of pests and plant diseases, and the remediation of soils (Silva and Rodrigues 2014; Silva et al. 2017; Theapparat et al. 2015; Togoro et al. 2014). Melo et al. (2017) found promising results in using pyroligneous liquor for the integrated management of plant diseases.

Campos et al. (2012) developed a phyto-protection and fertilizer formulation based on chitosan and pyroligneous distilled liquor with added minerals for use in agriculture. The formulation was able to induce resistance in plants. The pyroligneous liquor mentioned by the authors was a fraction collected between 80 and 150 °C from the smoke of carbon, with subsequent vacuum distillation.

Chitosan is a linear polysaccharide, which is biocompatible and non-toxic, and is composed of β-(1,4)-2-amino-2-deoxy-D-glucose and β-(1,4)-2-acetamide-2-deoxi-D-glucose units. Provided from a renewable source, this polysaccharide is obtained by the deacetylation of chitin, an abundant natural biopolymer, mainly extracted from the exoskeletons of various crustaceans (Dang et al. 2011; Kim et al. 2011). Chitosan, similarly to pyroligneous liquor, is obtained from a renewable source, biodegradable, and a multipurpose material. In agriculture, chitosan-based products have found applications as antimicrobial agents, antioxidants, and postharvest preservatives (Badawy and Rabea 2009; Di Piero and Garda 2008). Other important applications in pharmacology and medicine include drug delivery and fibers and fabrics in food packaging (Kara et al. 2016; Liu et al. 2013; Rong et al. 2016; Suresh et al. 2015). Chitosan combined with zeolite and bentonite has been proposed to remove from water organic compounds (Dehghani et al. 2017a) and heavy metals (Dehghani et al. 2017b, c), respectively.

The chitosan molecules, depending on the solvent system, may adopt different spatial arrangements and interact with several anionic species; their behavior in solution depends on the molar mass and degree of deacetylation, as well as on the pH of the medium (Babak et al. 2007; Lee et al. 2013; Shipovskaya et al. 2016).

The processing of chitosan systems can produce nanoparticles (Li and Huang 2012) or films (Porto 2011).

The characteristics of chitosan films are defined by a group of factors besides the molecular weight and deacetylation degree: it depends strongly on the preparation conditions (Yakunin et al. 2013).

Arabancita et al. (2015) observed that the antimicrobial properties of chitosan films depend on the pH of the precursor solution and films are more active in acidic pH. The authors found that the films inhibit the growth of Gram-positive and Gram-negative bacteria.

All of the studies above show the potential use of a formulation based on pyroligneous liquor and chitosan. The main purpose of this work is to characterize a formulation composed of chitosan and a fraction of distillation of pyroligneous liquor (DPL), resulting from the pyrolysis of *Eucalyptus grandis*. The present study was undertaken to evaluate the features of chitosan/DPL formulations through static and dynamic light scattering, pH and differential scanning calorimetry, rheology, and viscosity measurements. Auto-supported films obtained from these systems were characterized with respect to their properties of blocking UV-Vis radiation, swelling degree in water, thermal degradation, and water vapor permeability. The structural characteristics were obtained by X-ray diffraction (XRD), scanning electron microscopy (SEM), and Fourier transform infrared spectroscopy (FTIR).

Experimental details

Materials

The pyroligneous liquor was obtained through an extraction procedure of *Eucalyptus grandis* proposed by Campos (2018), in which the smoke and gases were collected in the range of temperatures between 80 and 150 °C. The pyrolysis liquor was stored for 6 months to be stabilized. After this, the product was distilled in a Buchi rotary evaporator, model R-114. The fraction collected in the temperature range from 60 to 75 °C was used in this work and is named distilled pyroligneous liquor. The DPL was then characterized by gas chromatography coupled to mass spectroscopy (GC/MS), FTIR, and proton nuclear magnetic resonance spectroscopy (^{1}H NMR).

The GC/MS was performed in a Shimadzu model QP 2010S equipped with a Restek RTX-5MS capillary column (30 m × 0.25 mm × 0.25 μm). The injector and detector temperatures were 250 and 220 °C, respectively. The heating was performed in the following steps: (a) an isothermal at 80 °C for 4 min; (b) heating up to 250 °C, with a heating rate of 6 °C min^{-1}; (c) isothermal at 250 °C for 10 min; (d) heating up

to 290 °C with a heating rate of 8 °C min^{-1}; and (e) isothermal at 290 °C for 12 min. The *split* ratio was 1/20 and gas flow in the column was 0.9 mL min^{-1}. Derivatization of distilled pyroligneous liquor was performed before injection. The water content was evaporated at a temperature lower than 50 °C (to avoid the loss of volatile compounds); the residue was dissolved in pyridine and silanized with a mixture of hexamethyldisilazane (HMDS) and trimethylchlorosilane (TMCS) 2:1. The data were analyzed with GC/MS LabSolutions® software. The identification of the compounds was performed by comparing the mass spectra obtained with the library NIST 2009.

The sample was dissolved in D_2O/HCl 0.1% (*v*/*v*) for ^{1}H-NMR; the spectrum was obtained in a Varian machine, model Innovate 300 MHz.

FTIR analyses of the distilled pyroligneous liquor took place in a KBr cell in an IR Prestique-21. The spectra were obtained with the transmittance mode, with the accumulation of 32 scans, between 4000 and 500 cm^{-1}, with a resolution of 4 cm^{-1}.

Chitosan was provided by Nutrifarm™ with 97% deacetylation degree, determined previously by proton magnetic resonance (Porto 2011).

Preparation and characterization of the precursor systems composed of chitosan/DPL

The solutions were composed of chitosan and DPL. These formulations were also used to prepare the chitosan auto-supported films, registered as green chemistry material at Instituto Nacional de Propriedade Intelectual in Brazil (PCT/BR2013/000597), in the USA (US20150336854 A1), and in Germany (DE112013006230T5) as a phyto-protector for use in agriculture.

Powdered chitosan was mixed with DPL in concentrations in the range from 0.05 to 10 g L^{-1}, which permitted a medium rate flow and could form smooth films. The systems were stirred for 2 h at room temperature.

Conductivity and pH measurements were obtained in Digimed Equipments, pH meter DM-20, and conductivimeter DM-31, respectively, and aimed to obtain information about the electrolytes dispersed in aqueous media.

Thermal characterization of the solution chitosan/DPL was observed by differential scanning calorimetry. The measurements were obtained in a DSC model Q 20-TA Instruments, in the temperature range from − 40 to 60 °C, at a heating rate of 10 °C min^{-1}, under N_2 flow of 50 mL min^{-1}.

The static (SLS) and dynamic (DLS) light scattering were undertaken with a Brookhaven Instruments goniometer, with He-Ne laser Brookhaven Instruments at 632.8 nm. The Zimm method was used and light scattering was measured at angles from 35° to 145°, with a 5° step, at 25 °C.

The Zimm plot was obtained in a range from 35° to 145°, with a 5° step. The SLS measurements were obtained in angles that varied from 75 to 105°, with a 2.5° step, an open filter, and a 1 mm slit. The DLS measurements took place at 90° with an open filter and 400 nm slit.

The increase in the refractive index as a function of concentration was obtained by the Brookhaven Instruments model BI-DNDC differential refractometer. The obtained solutions were filtered with a 0.45 μm pore hydrophilic filter directly for the optical cubets and subsequently centrifuged at 3000 rpm for 60 min to eliminate the possible interference of dust.

The rheological characterization was obtained in a Digital Brookfield model DV-II + PRO viscometer, with an ULA-EY apparatus. The shear stress measurements as a function of shear velocity were performed in 10.0 g L^{-1} chitosan solution, in a temperature range from 10 to 40 °C.

Due to the observed Newtonian behavior, it was possible to perform viscosity measurements through a Cannon Frenske viscometer. Chitosan/DPL solutions were studied in the concentration range from 0.05 to 30.0 g L^{-1}, at a temperature of 25 °C.

Preparation and characterization of the auto-supported chitosan/DPL films

Self-supported films of different thicknesses were obtained by dropping 20 mL solution into a 24 cm^2 area polyethylene support. The hydrogels were dried for 3 days at 40 °C. The films were characterized by FTIR, XRD, SEM, UV-Vis spectroscopy, thermal gravimetric analysis (TGA), swelling in water, and water vapor permeability.

FTIR analyses of the films were obtained in the transmittance mode, with the accumulation of 32 scans, between 4000 and 500 cm^{-1}, with a 4 cm^{-1} resolution.

XRD was performed with a Siemens *D500* diffractometer using θ–2θ geometry, containing Cu anode (Cu-Kα, λ = 1.541 Å). The scan was carried out varying 2θ from 2 to 50°, with a scan rate of 0.2°min^{-1}.

The morphology of the film surface was observed by SEM, performed with a Shimadzu model SSX-50 Superscan. The samples were fixed in a sample holder covered with carbon and a thin layer of gold (50 nm) was deposited on top to improve electrical conductivity. The samples were analyzed on top and with a cross-section to obtain the thickness.

The UV-Vis spectra of the films were obtained in the transmittance mode, from 200 to 800 nm, with a Shimadzu spectrophotometer (Model UV-1601 PC). The thicknesses of the films were evaluated with a digital micrometer.

The thermal stability of the films was determined through thermogravimetric analysis (TGA), carried out in a TGA50H, in the temperature range from 10 to 500 °C, at a heating rate of 10 °C min^{-1}, under a 50 mL min^{-1} N_2 flow.

Films with similar areas and thicknesses were weighed in an ATI CAHN C-35 balance, with a precision of 0.1 μg, immersed in distilled water, and dried and weighed at different immersion times up to 24 h. The average value of five determinations was taken for each immersion time.

The water vapor permeability of the chitosan films was determined by an adaptation of the American Society for Testing and Materials standard gravimetric method, E96-95 (ASTM 1995). Dry silica gel (Synth), 9 g previously dry, was placed in a 13-mL flask and covered with the chitosan films. Silicon glue was used at the glass/film interface and a rubber ring and aluminum seal were used to prevent the films from being released from the bottles, as described by Plotegher (2010). The systems were placed in a desiccator containing 250 mL of calcium chloride solution 10% (*w*/*w*), at 25 °C. Over 5 days, the samples were withdrawn and weighed regularly. The experiment was performed in quadruplicate.

Results and discussion

Chemical characterization of distilled pyroligneous liquor

The mass spectroscopy analysis was performed for each retention time, as shown in the chromatogram in Figure SM1 (see the Supplementary Material); it revealed the presence of different chemical species, including aromatic, phenolic, carbonylic, as well as organic compounds containing heteroatoms, as can be seen in Table 1. This result agrees with those reported in the literature (Mathew and Zakaria 2015; Pimenta et al. 2018; Souza et al. 2012).

The FTIR and ^{1}H NMR corroborate the results obtained by CG/MS, where the main chemical species present in DPL used in this work are aromatic or heteroaromatic compounds, carbonylic, phenolic, and carboxylic acids. In Fig. 1a, the FTIR DPL spectrum shows a very intense absorption band, due to the axial deformation of OH bonds (υ_{OH}) around 3360 cm^{-1}. DPL also presents some water content which makes the characterization of other chemical species in solution difficult. However, it is possible to observe two superimposed bands in the region between 1698 and 1626 cm^{-1}, which are attributed to $\upsilon_{C=O}$ (Silverstein and Webster 2000). The region with peaks between 1 and 3.5 ppm can be attributed to aliphatic hydrogen, and between 9 and 6 ppm can be attributed to aromatic and heteroaromatic compounds (Fig. 1b). The insert in Fig. 1b shows an amplification of the region between 6 and 10 ppm corresponding to phenolic hydrogen intramolecular bonds (Silverstein and Webster 2000).

Characteristics of chitosan/DPL solutions

The pH of the solutions slightly increased with the amount of chitosan, varying from 2.95 in DPL to 3.75 in the systems containing 30 g L^{-1} chitosan in DPL. This result suggests that these systems can have an improved antifungal effect (Tayel et al. 2010; Xiaolin et al. 2009).

The conductivity of the DPL/chitosan solutions permits to a deduction about the presence of dissolved electrolytes. Contrary to the usual behavior of polymeric solutions, this characteristic is important as it affects the conformation of polymer and the radium of hydration. For the system chitosan/DPL, in low chitosan concentrations, the increase in chitosan concentration is not followed with a significant increase in conductivity. However, at the highest concentrations, the ionization of chitosan groups led to an increase in the mobility of ions in solution and the conductivity grew significantly with chitosan concentration (Fig. 2). A similar behavior was also observed for polyelectrolyte solutions reported by Reiznautt et al. (2017).

We attribute a possible reason for this behavior to the presence of ionic species with chitosan and also to the ionization of the amine groups in DPL (as the observed pH is low).

Table 1 Main chemical compounds identified in the distilled pyroligneous liquor

Identified peak	Retention time (min)	Similarity (%)	Compound
1	3.817	84	Tetrahydropyran
2	4.833	96	3-Methyl-2-cyclopenten-1-one
3	5.050	98	Phenol
4	6.558	95	2,3-Dimethyl-2-cyclopenen-1-one
5	6.850	97	Phenol,2-methyl (ortho-cresol)
6	7.375	97	Phenol,3-methyl (meta-cresol)
7	7.842	98	Phenol,2-methoxy
8	9.275	93	Phenol,2,3-dimethyl (2,3-xylenol)
9	10.483	95	Para-cresol,2-methoxy
10	12.608	95	Phenol,4-ethyl-2-methoxy
11	14.300	90	Phenol-2,6-dimethoxy

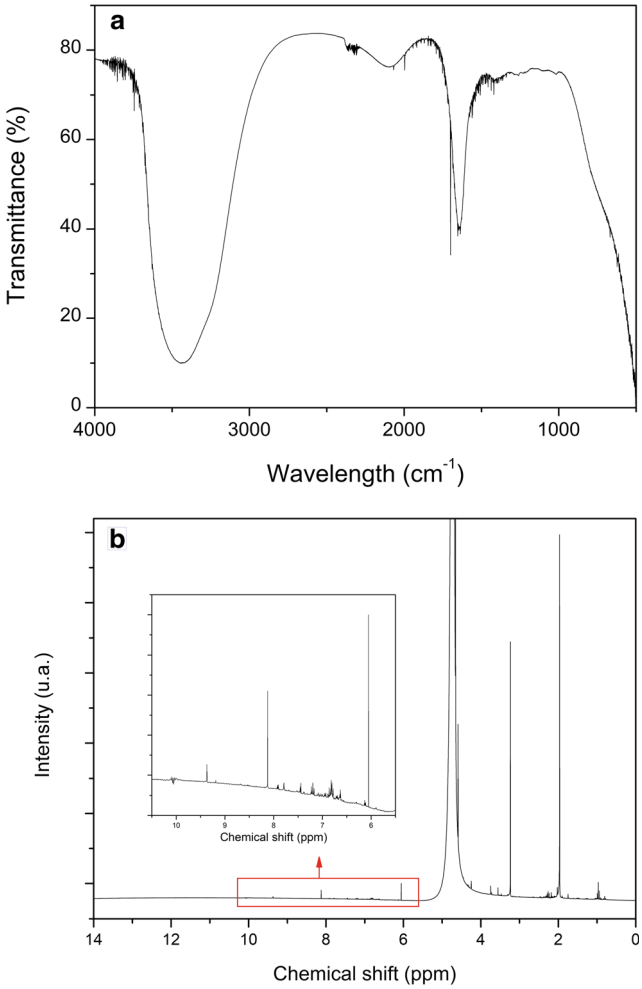

Fig. 1 **a** FTIR spectrum of DPL. **b** ^{1}H NMR of DPL

For systems with the opposite behavior of conductivity as a function of polymer concentrations, the critical aggregation concentration (c.a.c.) is estimated from the intersection between two straight lines obtained by linear regression (Villetti et al. 2011). If we consider this, just from the change in slope of the curves, the concentration for interception of the curves is 10.2 g L^{-1}.

In Fig. 3, the thermal behavior of the chitosan/DPL system is presented. A discontinuity at approximately 24 °C in the first heating curve cannot be seen in the second heating curve. This discontinuity can be attributed to the loss of water during the first heating (Nady and Kandil 2018). It was not possible to identify any phase transition in the range of temperatures studied. This is in agreement with the distillation process of the DPL previously described. The fraction obtained is stable and remains stable in the presence of chitosan.

The static light scattering measurements based on the Zimm method relate the intensity of the scattered light to the average molar mass (M_w), second virial coefficient (A_2), and radius of gyration (R_g), through the standard Eq. 1 (Brown 1994):

$$\frac{KC}{R(\theta,C)} = \frac{1}{M_w}\left[1 + \frac{q^2R_g^2}{3}\right] + 2A_2C \quad (1)$$

where $R(\theta,C)$ is the scattered light intensity (Rayleigh ratio), C is the polymer concentration, q is the scattering vector, θ is the scattering angle, λ is the wavelength of radiation in vacuum, and K is the optical constant (Eq. 2):

$$K = \frac{2\pi^2 n_0 \left(\frac{dn}{dC}\right)^2}{\lambda^4 N_A} \quad (2)$$

where N_A is the Avogadro's constant and dn/dC is the refractive index increasing with polymer concentration, which is $1.975 \times 10^{-1} \pm 2.10^{-6}$ L g^{-1} in this work. Table 2 shows the LS results of the studied system.

The chitosan/DPL systems presented a positive second virial coefficient, which indicates that the polymer/solvent

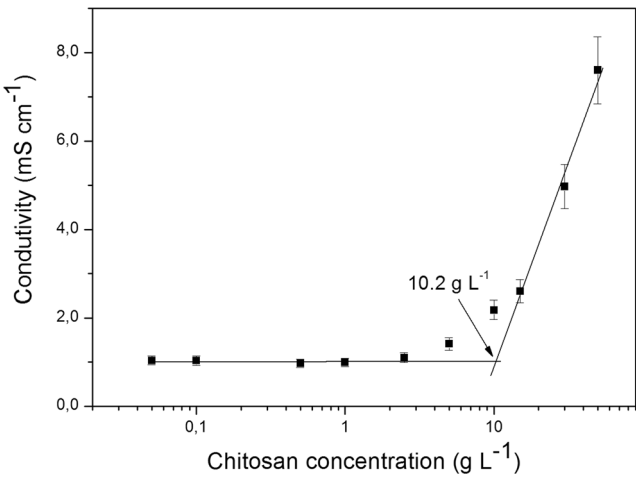

Fig. 2 Conductivity of chitosan/DPL systems as a function of chitosan concentration

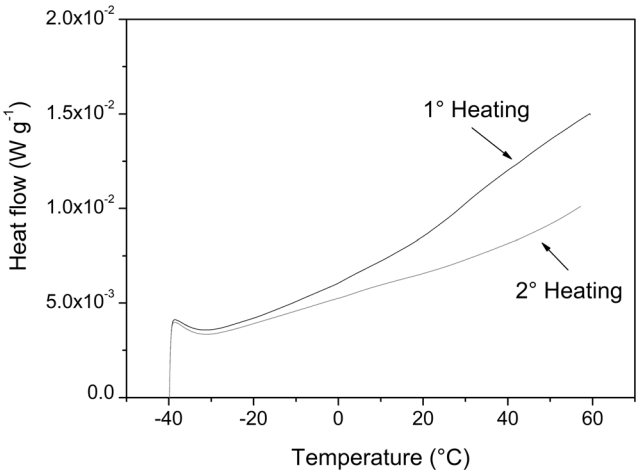

Fig. 3 DSC thermograms of chitosan/DPL at 10 °C min^{-1} heating rate

Table 2 Light scattering results obtained by the Zimm method for chitosan/DPL at 25 °C

Molar mass	$(1.029 \pm 0.16) \cdot 10^6$ g mol^{-1}
Second virial coefficient	$1.4 \pm 1.6 \cdot 10^{-5}$ cm^3 mol g^{-2}
R_g	153 ± 13 nm

interactions are favored. In fact, DPL can be considered as an excellent solvent for chitosan (Pohlmann et al. 2008). The organic compounds present in DPL interact with the chitosan amine groups and hydroxyl groups.

SLS results permit calculation of the gyration radius (R_g) of chitosan in DPL through dissymmetry of the static light scattering (Brown 1994). A curve of $R_g\ cos(\theta)$ versus $d(\theta)$ is exemplified in Figure SM2.

The values of R_g calculated by dissymmetry for chitosan/DPL systems for 0.1 and 1.0 g L^{-1}, at temperatures of 10 and 25 °C, are presented in Table 3.

The R_g value at 25 °C calculated by dissymmetry is very similar to that obtained by Zimm, 153 ± 13 nm. The tendency of R_g is to be reduced as the temperature decreases.

The dynamic light scattering (DLS) results has shown that only systems with chitosan concentrations higher than 0.05 g L^{-1} present a correlation function of 90°, at 25 and 40 °C. Figure 4 displays the normalized correlation function for 1.0 g L^{-1} at 25 and 40 °C, which present only one correlation time.

The chitosan solution is strongly solvated at 25 °C with an increase in temperature, the kinetic energy of the system increases and the molecules become poorly solvated. A consequence is an increase in mobility and the consequent shift of the curves for shorter relaxation times.

The treatment of the data obtained with angles varying from 35° to 135°, with steps of 15°, with the GENDIST software permitted to obtain the diffusion coefficient as a function of chitosan concentration. The value of the diffusion coefficient at infinite dilution, D_0, obtained by extrapolation of diffusion coefficient as a function of chitosan concentration, is 5.10^{-12} m^2 s^{-1} at 25 °C. The value of hydrodynamic radius at infinite dilution ($R_{h,}$) can also be obtained (Brown 1994) and is 42 nm.

Table 3 R_g obtained by dissymmetry for chitosan/DPL systems

Chitosan concentration (g L^{-1})	Temperature (°C)	R_g (nm)
0.1	10	86
0.1	25	133
1.0	10	81
1.0	25	107

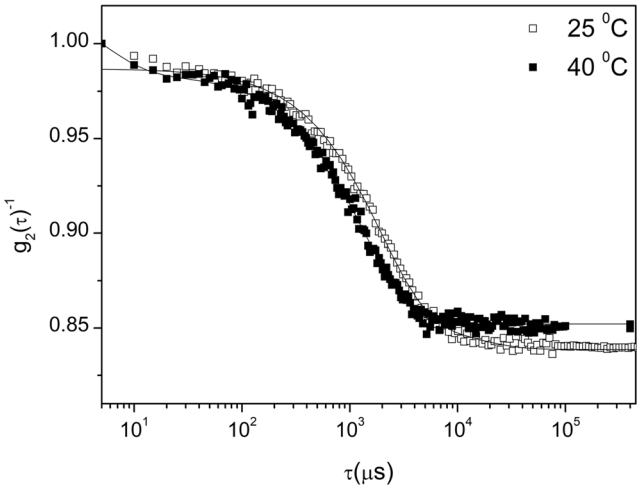

Fig. 4 Normalized correlation functions for 1.0 g L^{-1} chitosan /DPL system at 25 and 40 °C

The factor ρ factor, calculated according to Eq. 3, provides information about the conformation of the chitosan chains in solution.

$$\rho = \frac{R_g}{R_h} \tag{3}$$

The value of ρ is 3.64, which indicates that chitosan in DPL takes the conformation of rigid rod, corresponding to a good interaction of the molecules in solution (Pa and Yu 2001; Pohlmann et al. 2008).

The rheological characterization was performed with a 10 g L^{-1} chitosan system from 10 to 40 °C. Figure 5 shows the curves of shear tension as a function of shear rate for the solution 10.0 g L^{-1} chitosan in DPL at 10 and 40 °C. We observe that the hysteresis curve is more pronounced at low temperatures. It is also observed that the system presents Newtonian behavior in the range of the studied temperature.

It is possible to observe linearity between the shear tension and deformation rate, characteristic of a Newtonian fluid. The fitting according to Eq. 4 allowed the determination of the consistency index or apparent viscosity, b (Schifino 2013), according to Eq. 4:

$$\sigma = a + b \times \Upsilon^n \tag{4}$$

where σ is the shear tension, Υ is the shear rate, and a and n are the linear coefficient and the power-law coefficients, respectively. This was produced for a solution at 40 °C of 0.089, 0.08, and 0.96 for a, b, and n, respectively. At 10 °C, the values of a, b, and n were 0.03, 0.145, and 0.98, respectively. The value of n close to 1 and the small value of a show that the

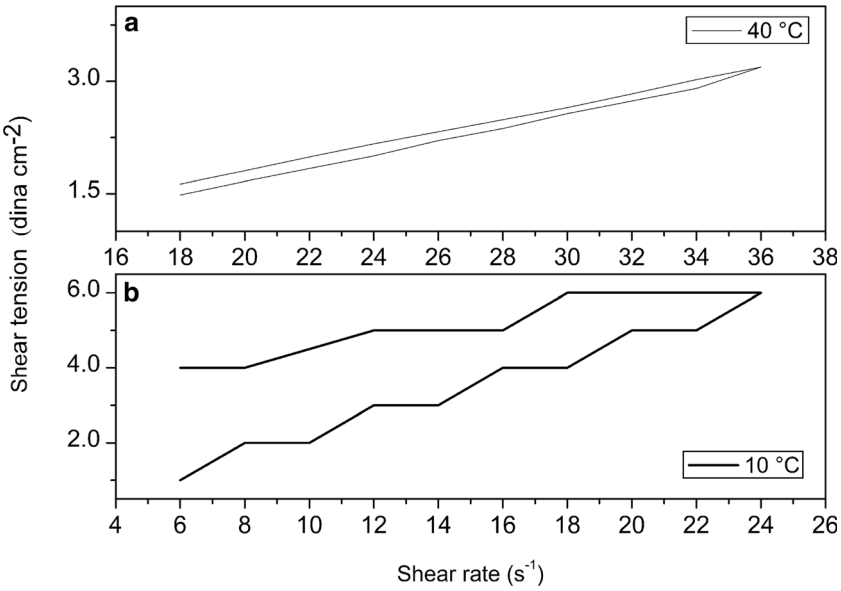

Fig. 5 Shear tension as a function of shear rate for 10 g L^{-1} chitosan in DPL at **a** 40 °C and **b** 10 °C

systems present characteristics of Newtonian fluids. The hysteresis at low temperature is more pronounced.

A similar behavior was observed for chitosan in acetic acid solution by Bazunova et al. (2015). The authors investigated the rheological properties and determined that the critical chitosan concentration for the formation of the fluctuation network in chitosan/acetic acid is 1.3 g L^{-1}. The addition of oppositely charged micelles to a semi-dilute chitosan solution results in solution structuration. This occurs due to the formation of an additional network consisting of polyelectrolyte complexes between polymer and colloidal particles.

Figure 6 shows the viscosity as a function of concentration at 25 °C for chitosan/DPL systems.

It is possible to observe the critical aggregation concentration (c.a.c.) for the system: 14.5 g L^{-1} for chitosan diluted in DPL. This value is very similar to the concentration for which the conductivity curves have shown an abrupt change in slope. In the face of these facts, we can affirm that this region of concentration can be interpreted as a c.a.c for chitosan in DPL.

The viscosity of a solution is affected by the molar mass and the shape of the molecule in solution. The shape of a polyelectrolyte molecule can be easily altered by changing the degree of dissociation and by increasing the ionic strength of the medium. As the ionic strength increases, the repulsive forces between the chains increase, presenting the rigid rod conformation, increasing the viscosity of the system (Pohlmann et al. 2008).

The viscosity values obtained for 10 g L^{-1} chitosan in DPL are presented in Fig. 7 as a function of temperature. The activation energy of viscous flow for the investigated

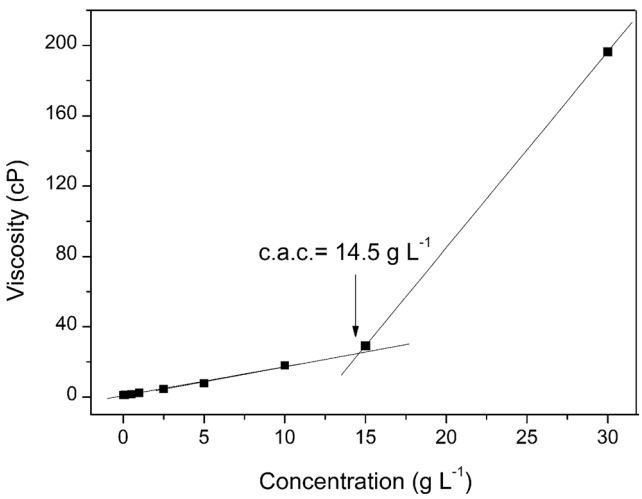

Fig. 6 Viscosity of chitosan/DPL system at 25 °C

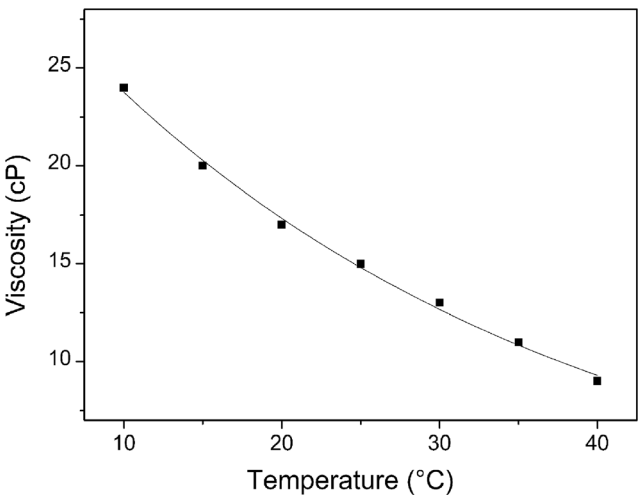

Fig. 7 Viscosity as a function of temperature for the system composed of 10.0 g L^{-1} chitosan in DPL

systems in the temperature range from 10 to 40 °C was estimated via Arrhenius–Frenkel–Eyring, also referred to in the literature as De Gusman Eq. (5) (Bazunova et al. 2015; Schifino 2013):

$$\eta = A.e^{\frac{Ea}{RT}} \quad (5)$$

where A is the pre-exponential factor, E_a is the activation energy of flow, R is the Regnault constant, and T is the absolute temperature (Bazunova et al. 2015). The calculated value of activation energy of flow is 23.16 kJ mol^{-1}.

Film characterization

The FTIR spectra of the chitosan powder and the film produced from chitosan solution are displayed in Fig. 8. A large absorption band is observed in the region from 3300 to 3500 cm^{-1}, which is characteristic of axial deformation of OH groups, superimposed to the axial deformation of amino groups. Aliphatic C–H was observed by ν_s and ν_{ass} at 2932 and 2890 cm^{-1}, respectively; the axial deformation of the C=O amide group is at 1650 cm^{-1} and the angular deformation of the NH group is at 1600 cm^{-1}. At 1417 cm^{-1}, there is absorption due to angular deformation of the NC group and the deformations of the CO bond are at 1100 cm^{-1}. These bands are in agreement with the reported data for this polymer (Ghosh and Ali 2012; Liu et al. 2013; Ocak 2018). A magnification of the band at 1110 cm^{-1} can be observed in chitosan and chitosan/DPL films, as well as the shift in carbonyl group absorption (C=O) for values between 1580 and 1520 cm^{-1}. This indicates that interactions occur between DPL and chitosan. Our findings are in agreement with those of Ghosh and Ali (2012) which were also attributed to the intensification of the carbonyl bands, as well as a shift in C=O and NH deformation bands, to the chitosan/organic acid interaction.

The X-ray diffraction of the films (Fig. 9) shows peaks at 2θ, 8.4–8.6, and 11.55°, located on a broad halo characteristic of amorphous materials. This result is similar to that found by Nady and Kandil (2018) for chitosan films diluted in acetic acid, confirming that chitosan is a semi-crystalline polysaccharide. The degree of crystallinity still depends on the degree of deacetylation of chitosan. The higher the degree of deacetylation, the more favorable the polymer matrix for the formation of hydrogen bonds, and consequently the greater the degree of crystallinity observed (Liu et al. 2013; Yuan et al. 2011). This semi-crystalline characteristic is interesting for the development of coatings, as it gives the film flexibility, a desirable characteristic in the processes of water penetration and gas exchange.

The films obtained at different concentrations presented a uniform surface, without the presence of bubbles, and were smoother at lower chitosan concentrations (Fig. 10). The micrographs show a homogeneous and compact structure similar to the data found in other works with this polymer (Liu et al. 2013; Nady and Kandil 2018; Ocak 2018).

The films were characterized with respect to their transparency to UV-Vis radiation. A typical UV-Vis spectrum of chitosan/DPL is presented in Fig. 11a. Due to the low transmittance observed in the region between 200 and 320 nm, films can act as sun blockers in the ultraviolet region, UVC (297–100 nm) and UVB (319–280 nm), of the electromagnetic spectrum. The molar absorptivity can be calculated for different wavelengths (λ), when the thickness of the films is known, through the Lambert-Beer law adapted to auto-supported films (Eq. 6):

$$A(\lambda) = \varepsilon(\lambda)bc \quad (6)$$

where A (λ) and ε (λ) are the absorbance and the molar absorptivity (L mol^{-1} cm^{-1}) of the films as a function of

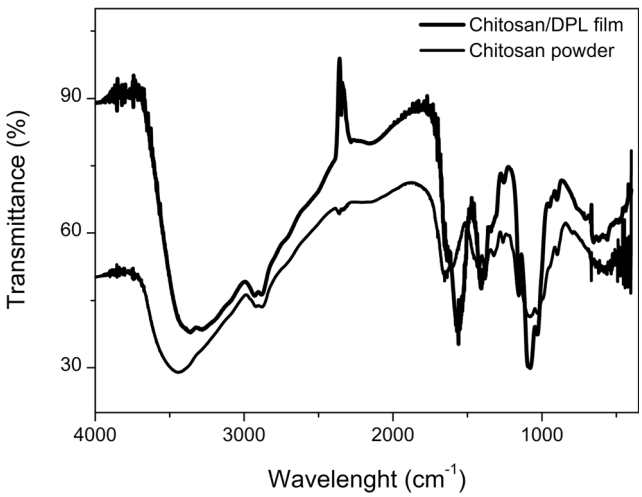

Fig. 8 FTIR spectra of the chitosan/DPL film and pure chitosan

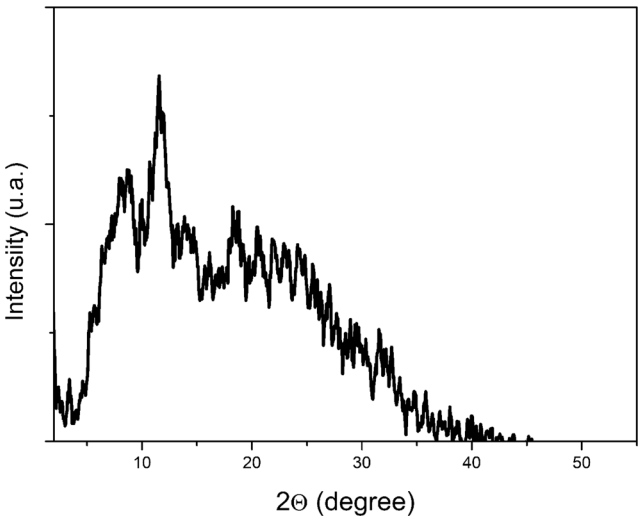

Fig. 9 X-ray diffractogram of chitosan/DPL = 0.1542 nm

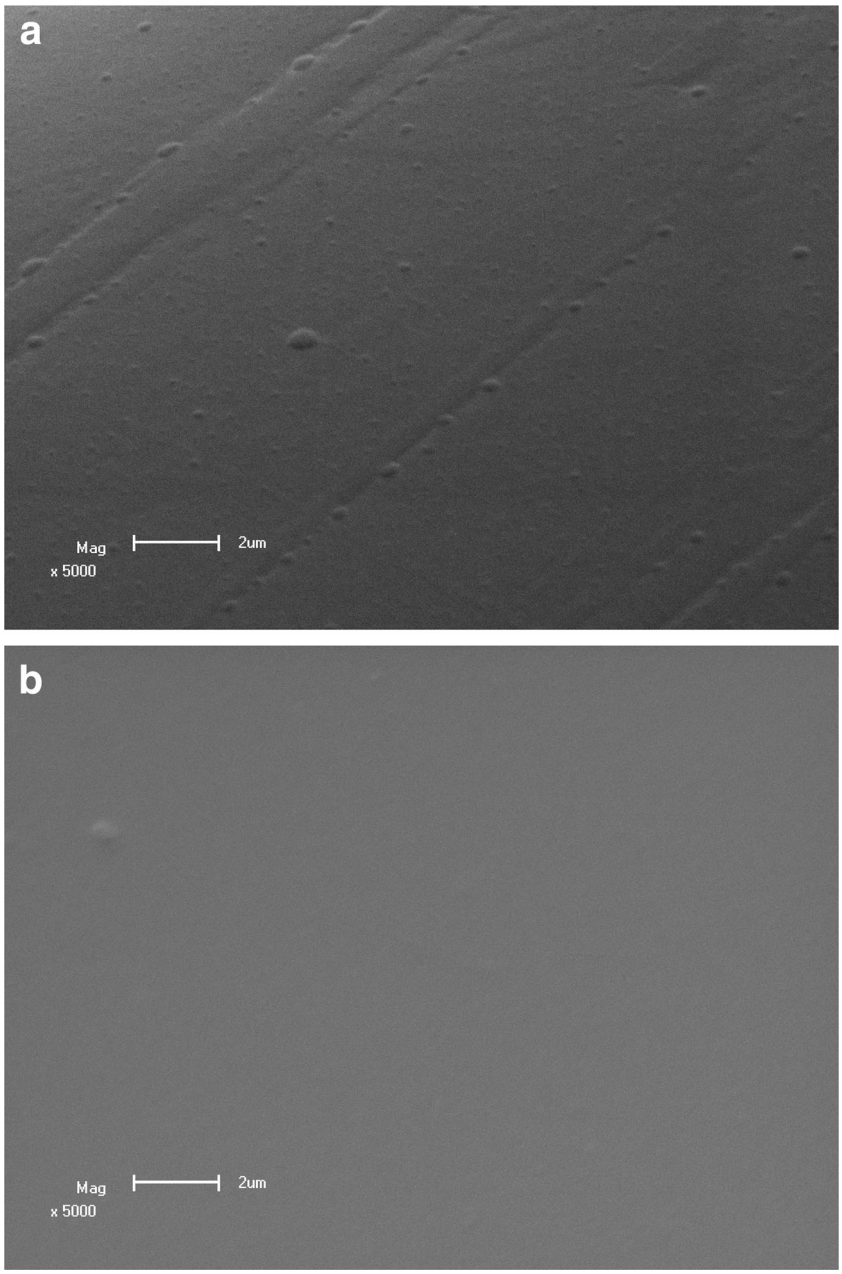

Fig. 10 Scanning electron microscopy of the films of chitosan/liquor pyroligneous distilled 0.5 g L^{-1} (**a**) and 10 g L^{-1} chitosan (**b**)

wavelength, respectively; b is the film thickness (cm); and c is the chitosan concentration (mol L^{-1}). The thickness of the films was determined by measuring the cross-sections with SEM. The molar absorptivity as a function of the wavelength is shown in Fig. 11b and the fitting is expressed through Eq. 7:

$$\varepsilon = 4.6 \times 10^8 \exp(-\lambda/100) + 1.4 \times 10^6 \quad (7)$$

The decrease in absorptivity with wavelength permits the formulation of films with different thicknesses and concentrations, according to the desired blocking effect.

Thermal stability of the films, evaluated by TGA curves, is shown in Fig. 12. DPL/chitosan film is stable up to 45 °C when it loses about 20% of its weight, which is attributed to the water releasing in a structure. At 300 °C, the process of degradation starts in the film and 40% in weight of amorphous carbon remains at the end of the pyrolysis process.

Similar data were obtained by Fráguas et al. (2015) for chitosan-based comestible films.

The swelling measurements provide information about the affinity between the films and water; this is important for hydration purposes. The degrees of swelling as a function of time are obtained through the Eq. (8):

$$\Delta m = \left(\frac{m_i - m_0}{m_0}\right) * 100 \quad (8)$$

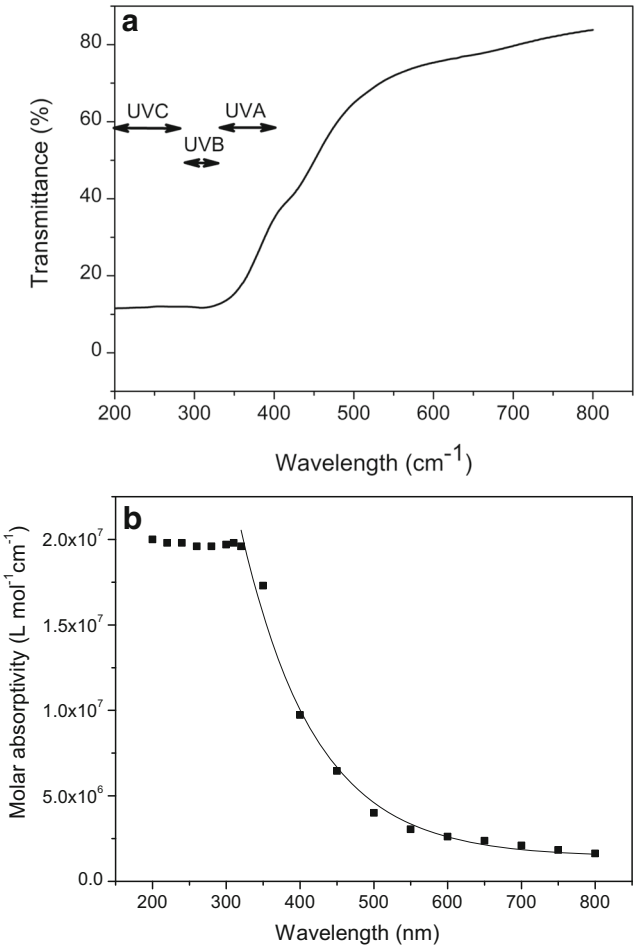

Fig. 11 **a** Transmittance as a function of wavelength for 20 μm chitosan/DPL film (10 g L^{-1}) with 47 μm thickness. **b** Molar absorptivity of chitosan films as a function of wavelength at 25 °C

where Δm (expressed as % in weight) is the relative weight increase, m_0 is the initial mass of the film, and m_i is the mass measured after the immersion time i.

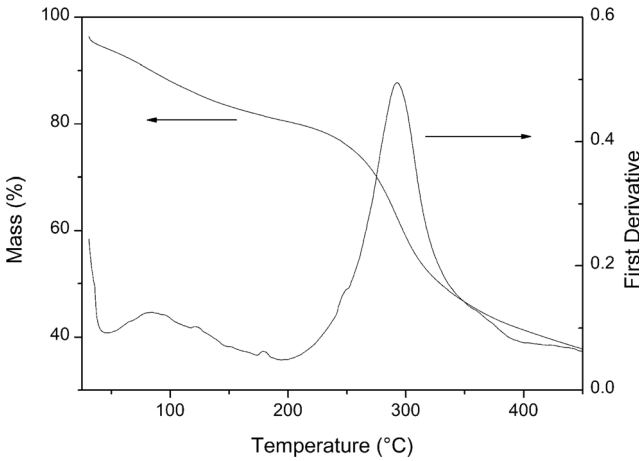

Fig. 12 Thermal gravimetric profile and first derivative of the DPL/chitosan

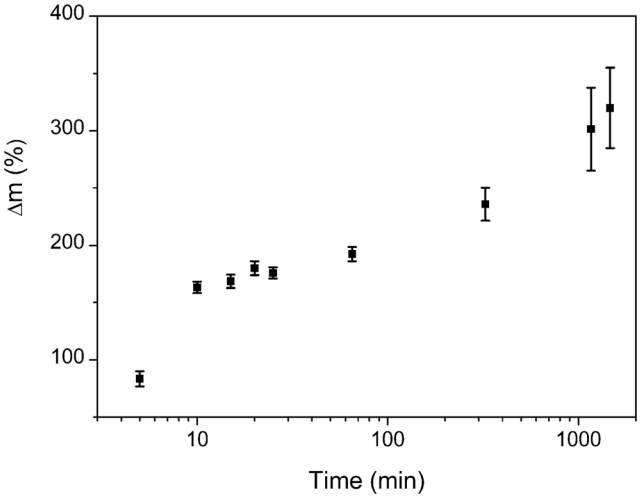

Fig. 13 Variation in the relative weigh of the chitosan/DPL films, after immersion in water as a function of immersion time, at 25 °C

The results shown in Fig. 13 were obtained by averaging five determinations for each time, over a period of 24 h. It could be observed that the films remained stable where immersed in water for up to 7 days. This behavior is in agreement with the low solubility of chitosan in water.

These films present high hygroscopicity but the dissolution rate is very slow and its behavior can be explained by the crosslinking between chitosan chains promoted by DPL.

Results of the permeability experiments to water vapor can be seen in Fig. 14. The DPL/chitosan films are permeable to water vapor and the increase in thickness is responsible for a decrease in permeability according to the law expressed by Eq. (9):

$$WVP\left(\mathrm{g\ m^{-2}\ h^{-1}}\right) = 45.74 - 0.19 * t(\mu\mathrm{m}) \quad (9)$$

According to Vimaladevi et al. (2015), the diffusion of water vapor in chitosan films is affected significantly by

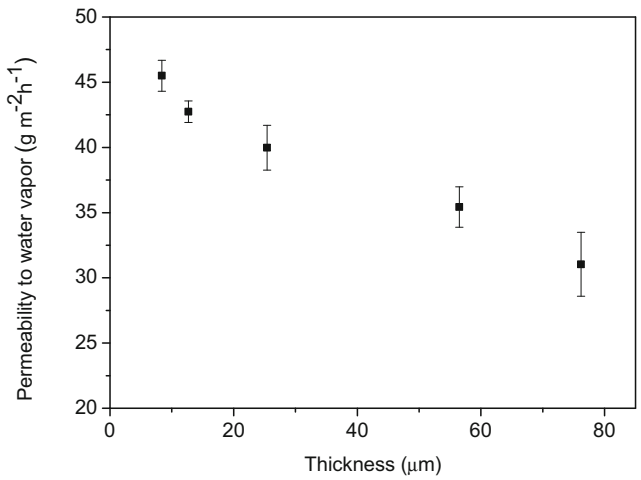

Fig. 14 Permeability to water of films obtained from solutions at 0.5, 1, 3, 5, and 10 g L^{-1} chitosan in DPL

the pH of the precursor chitosan solution and the nature of the acid used.

Concluding remarks

In this work, we characterized the physicochemical properties of chitosan solubilized in distilled pyroligneous liquor and the films obtained from those systems.

Distilled PL can be considered a raw material obtained from renewable sources, and is a good solvent for chitosan. The solution is stable up to 60 °C, the chains are in a rod rigid conformation, and the flow follows Newton's law. The activation energy of flow is 26 kJ mol^{-1} and the critical aggregation concentration was determined to be 14 g L^{-1}.

The films obtained from this solution by casting showed a semi-crystalline structure, which is smooth and stable up to 50 °C, because it loses less than 5% in weight, which permits its use in environmental conditions.

DPL/chitosan films are permeable to water vapor and present high hygroscopicity. The obtained films are able to efficiently block the incident UVB and UVC radiation and the molar absorptivity decreases exponentially with increasing wavelength.

The cationic properties of chitosan and the composition of DPL confer to the films obtained from the desirable properties of these precursors with regard to being used as coatings. In addition, the antioxidant and antimicrobial properties reported of the precursors show that it can be a potential for several applications.

Acknowledgements The authors thank Conselho Nacional de Pesquisa—CNPq (Proc. 311736/2015-7) and Vegetal Physiology Laboratory of EMBRAPA Clima Temperado.

References

Almeida RSR, Taccini MM, Moura LF, Ceribelli UL, Brito JO, Glória EM (2017a) Potential of pyroligneous extract of Eucalyptus wood as a preservative of cosmetic and sanitizing products. Waste Biomass Valoriz. https://doi.org/10.1007/s12649-017-0125-5

Almeida RSR, Taccini MM, Moura LF, Ceribelli UL, Brito JO, Millan M (2017b) Effect of storage time on the chemical characterization of pyroligneous liquor from Eucalyptus wood. Waste Biomass Valoriz. https://doi.org/10.1007/s12649-017-0067-y

Arabancita MY, López-Caballero ME, Gómez-Guillén MC, Fernández-Garcá M, Fernández-Martín F, Montero P (2015) Antimicrobial and rheological properties of chitosan as affected by extracting conditions and humidity exposure. LWT Food Sci Technol 60:802–810. https://doi.org/10.1016/j.lwt.2014.10.019

ASTM - American Society for Testing and Materials (1995) ASTM standard test methods for determining gas permeability characteristics of plastic film and sheeting. ASTM, Philadelphia

Babak VG, Auzely R, Rinaudo M (2007) Effect of electrolyte concentration on the dynamic surface tension and dilational viscoelasticity of adsorption layers of chitosan and dodecyl chitosan. J Phys Chem B 111:9519–9529 https://pubs.acs.org/doi/abs/10.1021/jp0718653

Badawy MEI, Rabea EI (2009) Potencial of the biopolymer with different molecular weights to control postharvest gray mold of tomato fruit. Postharvest Biol Technol 51:110–117. https://doi.org/10.1016/j.postharvbio.2008.05.018

Bazunova MV, Valiev DR, Chernova VV, Kulish EI (2015) Rheological properties of solutions of chitosan and its complexes with colloid particles of a silver iodide sol. Polym Sci Ser A 57:675–679. https://doi.org/10.1134/S0965545X15050041

Brown W (1994) Light scattering: principals and development. Clarendon Press, Oxford

Campos AD (2018) Processo de coleta e produção de extrato pirolenhoso para uso agrícola. Technical document 178, Embrapa Clima Temperado, Pelotas (in portuguese). https://ainfo.cnptia.embrapa.br/digital/bitstream/item/177829/1/Angela-Diniz-Campos-Circular-178.pdf

Campos AD, Ueno B, Porto FGS, Antunes IF, Garcia ITS, Pereira JFM, Castro LAS, Scivittaro WB (2012) Processo de obtenção de formulação com capacidade fertilizante e fitoprotetora, Formulação com capacidade fertilizante e fitoprotetora, Uso da formulação com capacidade fertilizante e fitoprotetora. Registered at Instituto Nacional de Propriedade Intelectual in Brazil (PCT/BR2013/000597), In United States (US20150336854 A1) and in Germany (DE112013006230T5)

Dang QF, Yan JQ, Li JJ, Cheng XJ, Liu CS, Chen XG (2011) Controlled gelation temperature, pore diameter and degradation of a highly porous chitosan-based hydrogel. Carbohydr Polym 83:171–178. https://doi.org/10.1016/j.carbpol.2010.07.038

Daroit D, Moura ABD, Martins IPD (2013) Vegetable charcoal and pyroligneous acid: technological, economical and legal aspects of its production and commerce. J Technol Manag Innov 8:310–320. https://doi.org/10.4067/S0718-27242013000300028

Dehghani MH, Dehghan A, Alidadi H, Dolatabadi M, Mehrabpour M, Converti A (2017a) Removal of methylene blue dye from aqueous solutions by a new chitosan/zeolite composite from shrimp waste: kinetic and equilibrium study. Korean J Chem Eng 34:1699–1707. https://doi.org/10.1007/s11814-017-0077-2

Dehghani MH, Zarei A, Mesdaghinia A, Nabizadeh R, Alimohammadi M, Afsharnia M (2017b) Adsorption of Cr(VI) ions from aqueous systems using thermally sodium organo-bentonite biopolymer composite (TSOBC): response surface methodology, isotherm, kinetic and thermodynamic studies. Desalin Water Treat 85:298–312. https://doi.org/10.5004/dwt.2017.21306

Dehghani MH, Zarei A, Mesdaghinia A, Nabizadeh R, Alimohammadi A, Afsharnia M (2017c) Response surface modeling, isotherm, thermodynamic and optimization study of arsenic (V) removal from aqueous solutions using modified bentonite-chitosan (MBC). Korean J Chem Eng 34:757–767. https://doi.org/10.1007/s11814-016-0330-0

Di Piero RM, Garda MV (2008) Quitosana reduz a severidade da antracnose e aumenta a atividade de glucanase em feijoeiro-comum. Pesq Agrop Brasileira 43:1121–1128. https://doi.org/10.1590/S0100-204X2008000900004

Fráguas RM, Simão AA, Faria PV, Queiroz ER, Oliveira EN Jr, CMP A (2015) Preparation and characterization of chitosan edible films. Polímeros 25:48–53. https://doi.org/10.1590/0104-1428.1656

Furtado CM, Stolz AS, Pinto FL, Moura ABD, Morisso FDP, Pitarelo AP, Ramos LP, Mühlen CV, Riegel-Vidotti IC (2015) Pyroligneous liquor produced from *Acacia mearnsii* de wild wood under controlled conditions as a renewable source of chemicals. Quim Nova 38:1068–1074. https://doi.org/10.5935/0100-4042.20150120

Ghosh A, Ali MA (2012) Studies on physicochemical characteristics of chitosan derivatives with dicarboxylic acids. J Mater Sci 47:1196–1204. https://doi.org/10.1007/s10853-011-5885-x

Kara HH, Xiao FG, Sarker M, Jin TZ, Sousa AMM, Liu CK, Tomasula PM, Liu LS (2016) Antibacterial poly(lactic acid) (PLA) films grafted with electrospun PLA/allyl isothiocyanate fibers for food packaging. J Appl Polym Sci 133:42475. https://doi.org/10.1002/app.42475

Kim KW, Min BJ, Kim YT, Kimmel RM, Cooksey K, Park SI (2011) Antimicrobial activity against foodborne pathogens of chitosan biopolymer films of different molecular weights. LWT Food Sci Technol 44:565–569. https://doi.org/10.1016/j.lwt.2010.08.001

Lee DW, Lim C, Israelachvili JN, Hwang DS (2013) Strong adhesion and cohesion of chitosan in aqueous solutions. Langmuir 29:14222–14229 https://pubs.acs.org/doi/10.1021/la403124u

Li J, Huang Q (2012) Rheological properties of chitosan-tripolyphosphate complexes: from suspensions to microgels. Carbohydr Polym 87:1670–1677. https://doi.org/10.1016/j.carbpol.2011.09.074

Liu M, Zhou Y, Zhang Y, Yu C, Cao S (2013) Preparation and structural analysis of chitosan films with and without sorbitol. Food Hydrocoll 33:186–191. https://doi.org/10.1016/j.foodhyd.2013.03.003

Lohri CR, Diener S, Zabaleta I, Mertenat A, Zurbrügg C (2017) Treatment technologies for urban solid biowaste to create value products: a review with focus on low- and middle-income settings. Rev Environ Sci Biotechonol 16:81–130. https://doi.org/10.1007/s11157-017-9422-5

Mathew S, Zakaria ZA (2015) Pyroligneous acid—the smoky acidic liquid from plant biomass. Appl Microbiol Biotechnol 99:611–622. https://doi.org/10.1007/s00253-014-6242-1

Melo TA, Araújo MUP, Serra IMRS, Pascholati SF (2017) Produtos naturais disponíveis comercialmente induzem o acúmulo de fitoalexinas em cotilédones de soja e mesocótilos de sorgo. Summa Phytopathol 43:205–211. https://doi.org/10.1590/0100-5405/167358

Nady N, Kandil SH (2018) Novel blend for producing porous chitosan-based films suitable for biomedical applications. Membranes 8:1–18. https://doi.org/10.3390/membranes8010002

Ocak B (2018) Film-forming ability of collagen hydrolysate extracted from leather solid wastes with chitosan. Environ Sci Pollut Res 25:4643–4655. https://doi.org/10.1007/s11356-017-0843-z

Pa J, Yu L (2001) Light scattering study of chitosan in acetic acid aqueous solutions. Macromol Chem Phys 202:985–991. https://doi.org/10.1002/1521-3935(20010401)202:7<985::AID-MACP985>3.0.CO;2-2

Pereira EG, Martins MA, Pecenka R, Carneiro ACO (2017) Pyrolysis gases burners: sustainability for integrated production of charcoal, heat and electricity. Renew Sust Energ Rev 75:592–600. https://doi.org/10.1016/j.rser.2016.11.028

Pimenta AS, Fasciotti M, Monteiro TVC, Lima KMG (2018) Chemical composition of pyroligneous acid obtained from Eucalyptus GG100 clone. Molecules 23:426–438. https://doi.org/10.3390/molecules23020426

Plotegher F (2010) Desenvolvimento de compósitos poliméricos baseados em matriz biodegradável e nanozeólitas. Dissertação, Universidade Federal de São Carlos (in Portuguese)

Pohlmann AR, et al. (2008) Tópicos em Nanociência e Nanotecnologia: II Mostra CNANO UFRGS. Editora Universidade Federal do Rio Grande do Sul, Porto Alegre (in Portuguese)

Porto FGS (2011) Caracterização de quitosana em ácido pirolenhoso destilado com potencial uso como coberturas protetoras. Dissertação, Universidade Federal de Pelotas (in Portuguese)

Reiznautt QB, Garcia ITS, Furlanetto BG, Angeloni LM, Samios D (2017) Copper removal from aqueous solutions using a polyelectrolyte derived from sunflower oil: physicochemical aspects. J Environm Chem Eng 5:5512–5520. https://doi.org/10.1016/j.jece.2017.10.039

Rong Q, Feng F, Ma Z (2016) Metal ions doped chitosan–poly(acrylic acid) nanospheres: synthesis and their application in simultaneously electrochemical detection of four markers of pancreatic cancer. Biosens Bioelectron 75:148–154. https://doi.org/10.1016/j.bios.2015.08.041

Schifino J (2013) Tópicos de Físico Química. Editora Universidade Federal do Rio Grande do Sul, Porto Alegre (in Portuguese)

Shipovskaya AB, Abramov AY, Pyshnograi GV, Aziz AJHN (2016) Rheological properties of aqueous acid solutions of chitosan: experiment and calculations of the viscometric functions on the basis of a mesoscopic model. J Eng Phys Thermophys 89:642–651. https://doi.org/10.1007/s10891-016-1422-8

Silva VC, Rodrigues CM (2014) Natural products: an extraordinary source of value-added compounds from diverse biomasses in Brazil. Chem and Biol Technol Agric 1(14). https://doi.org/10.1186/s40538-014-0014-0

Silva CJ, Karsburg IV, Dias PC, Arruda TPM (2017) Pyroligneous liquor effect on *in* and *ex vitro* production of *Oeceoclades maculata* (Lindl) Lindl. Rev Caatinga 30:947–954. https://doi.org/10.1590/1983-21252017v30n415rc

Silverstein RM, Webster FX (2000) Identificação Espectrofotométrica de Compostos Orgânicos. LTC, Rio de Janeiro (in Portuguese)

Souza JBG, Ré-Poppi N, Raposo JL Jr (2012) Characterization of pyroligneous acid used in agriculture by gas chromatography-mass spectrometry. J Braz Chem Soc 23:610–617. https://doi.org/10.1590/S0103-50532012000400005

Suresh PV, Raj KR, Nidheesh T, Pal GK, Sakhare PZ (2015) Application of chitosan for improvement of quality and shelf life of table eggs under tropical room conditions. J Food Sci Technol 52:6345–6354. https://doi.org/10.1007/s13197-015-1721-7

Tayel AA, Moussa S, Opwis K, Knittel D, Schollmeyer E, Hartfiel AN (2010) Inhibition of microbial pathogens by fungal chitosan. Int J Biol Macromol 47:10–14. https://doi.org/10.1016/j.ijbiomac.2010.04.005

Theapparat Y, Chandumpai A, Leelasuphakul W, Laemsak N (2015) Pyroligneous acids from carbonization of wood and bamboo: their components and antifungal activity. J Trop For Sci 27:517–526 http://www.jstor.org/stable/43596228

Togoro AH, Silva JAS, Cazetta OJ (2014) Chemical changes in oxisol treated with pyroligneous acid. Ciênca e Agrotec 38:113–121. https://doi.org/10.1590/S1413-70542014000200002

Villetti MA, Bica CID, Garcia ITS, Pereira FV, Ziembowicz FI, Kloster CL, Giacomelli C (2011) Physicochemical properties of methylcellulose and dodecyltrimethylammonium bromide in aqueous medium. J Phys Chem B 115:5868–5876. https://doi.org/10.1021/jp110247r

Vimaladevi S, Panda SK, Xavier KAM, Bindu J (2015) Packaging performance of organic acid incorporated chitosan films on dried anchovy (*Stolephorus indicus*). Carbohydr Polym 127:189–194. https://doi.org/10.1016/j.carbpol.2015.03.065

Xiaolin T, Dafeng T, Zhongyan MF (2009) Synthesis and evaluation of chitosan-vitamin C eomplexes. J Appl Polym Sci 114:2986–2991. https://doi.org/10.1002/app.30918

Yakunin NA, Losev NV, Lipatova IM (2013) Influence of mechanical treatment on the structure and properties of chitosan solutions and films based on them. Fibre Chem 45:19–23. https://doi.org/10.1007/s10692-013-9513-1

Yuan Y, Chesnutt BM, Haggard WO, Bumgardner JD (2011) Deacetylation of chitosan: material characterization and *in vitro* evaluation via albumin adsorption and pre-osteoblastic cell cultures. Materials 4:1399–1416. https://doi.org/10.3390/ma4081399

Distilled piroligneous liquor obtained from *Eucalyptus grandis* and chitosan: physical chemical properties of the solution and films

Fabiane Grecco da Silva Porto[1] e Ângela Diniz Campos[1], Irene Teresinha Santos Garcia[2*]

[1] *Laboratório de Fisiologia Vegetal, Embrapa Clima Temperado, Br 392, Km 78, caixa postal 403, 96010-971, Pelotas, Brasil*

[2] *Departamento de Físico-Química, Instituto de Química, Universidade Federal do Rio Grande do Sul, Avenida Bento Gonçalves 9500, 91501-970, Porto Alegre, Brasil*

*Corresponding author:

Irene Teresinha Santos Garcia

Supplementary Material

The GC/MS permitted to characterize the main components of distilled pyroligneous liquor (DPL). In Figure SM1 the chomatogram can be seen.

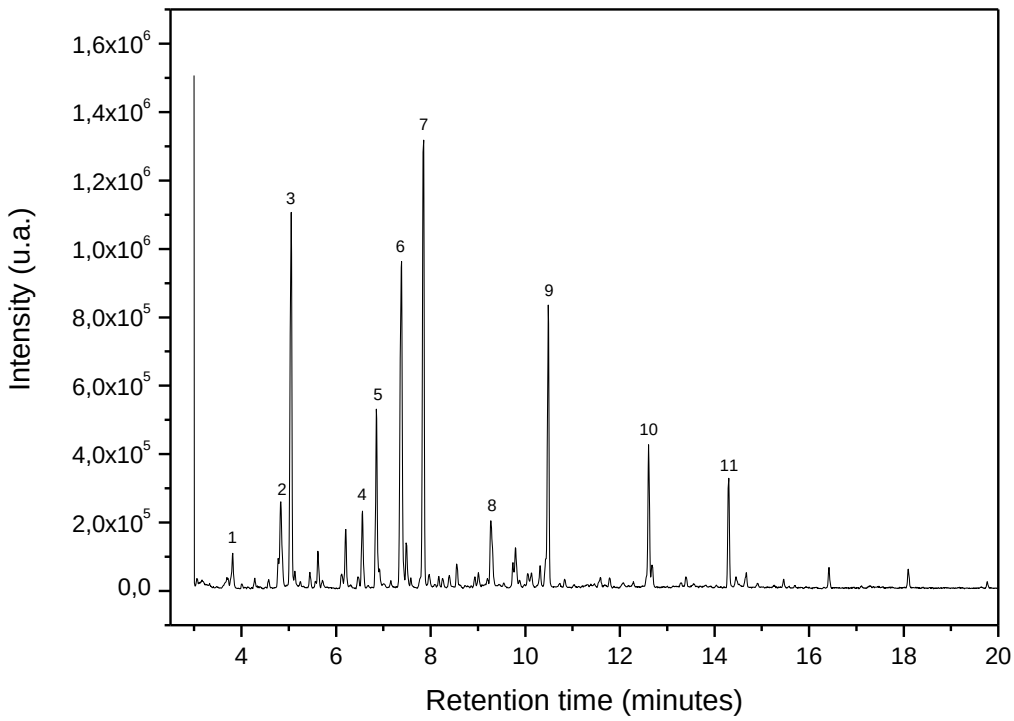

Figure SM1. Chromatogram of the distilled pyroligneous liquor.

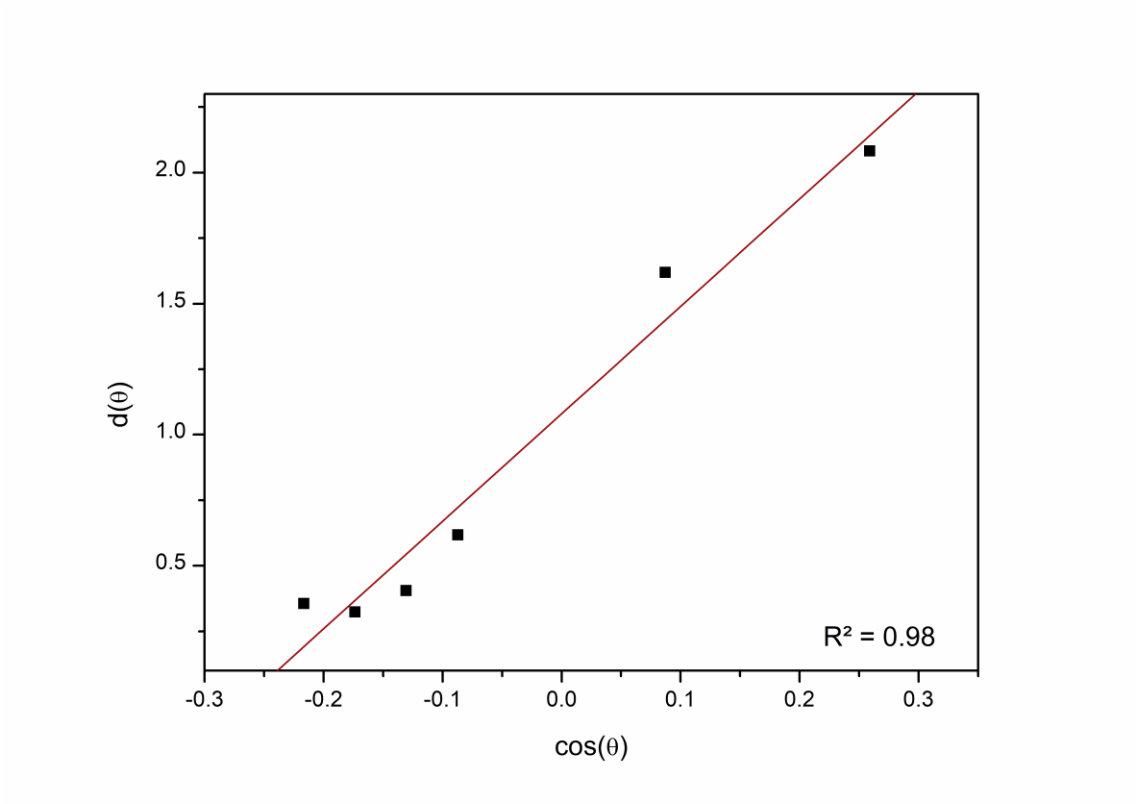

Dissimetry Curves of chitosan/DPL can be seen in Figure SM2.

Figure SM2. Relation between *cos(θ)* and *d(θ)* for 0.1 g L^{-1} chitosan in DPL at 25 °C.